**Supporting Information Figures**

A Patient-Friendly 16-Channel Transmit/ 64-Channel Receive Array Coil for Combined Head-Neck Magnetic Resonance Imaging at 7 Tesla

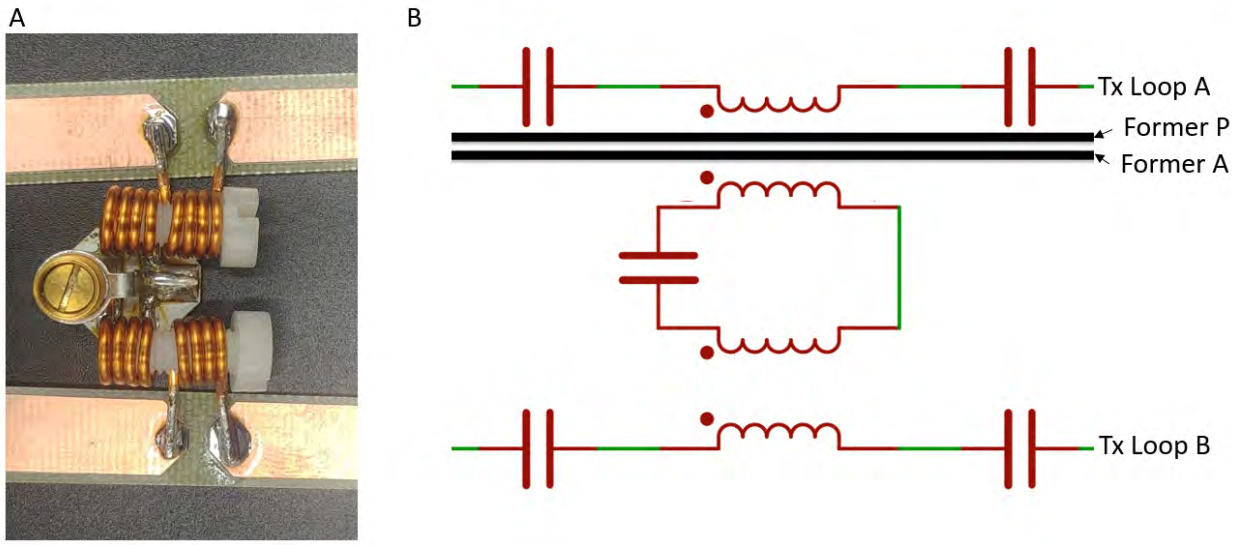


**FIGURE S1**: Schematic and implementation of the resonant inductive decoupling (RID) structure to be used for isolating adjacent Tx coil pairs. This decoupling structure was also used to decouple direct neighboring elements across the split housing segments on different formers. In this case, the Former P illustrates the represents of the posterior coil former where Former A is the anterior former.

A

| Channel | 1 | 2 | 3 | 4 | 5 | 6 | 7 | 8 | 9 | 10 | 11 | 12 | 13 | 14 | 15 | 16 |
|---|---|---|---|---|---|---|---|---|---|---|---|---|---|---|---|---|
| 1 | -26,17 | -28 | -31,16 | -44,15 | -31,41 | -34,56 | -39,68 | -39,01 | -39,56 | -35,21 | -33,59 | -25 | -44,87 | -44,65 | -46,18 | -34,56 |
| 2 | | -46,98 | -28,99 | -24,88 | -29,04 | -25,26 | -27,79 | -39,03 | -34,45 | -30,55 | -35,73 | -26,76 | -45,04 | -45,7 | -31,46 | -34,68 |
| 3 | | | -37,28 | -15,79 | -37,62 | -26 | -25,69 | -31 | -27,43 | -32,38 | -35,02 | -34,34 | -38,56 | -39,14 | -38 | -38,03 |
| 4 | | | | -33,1 | -41,68 | -31,62 | -25,59 | -39,08 | -15,09 | -34,56 | -39,8 | -31,96 | -41,98 | -46,89 | -37,33 | -42,83 |
| 5 | | | | | -26,67 | -21,47 | -26,15 | -41,67 | -47,9 | -36,66 | -37,03 | -38,14 | -44,45 | -33,72 | -28,08 | -29,08 |
| 6 | | | | | | -29,45 | -35,61 | -33,21 | -50,06 | -41,99 | -42,28 | -39,45 | -58,81 | -38,33 | -33,8 | -42,7 |
| 7 | | | | | | | -31,38 | -19,82 | -38,27 | -44,02 | -48 | -44,58 | -42,69 | -43,68 | -51,07 | -52,52 |
| 8 | | | | | | | | -34,74 | -30,94 | -51,24 | -43,65 | -37,74 | -25,66 | -27,68 | -29,49 | -44,98 |
| 9 | | | | | | | | | -38,03 | -29,62 | -30,93 | -32,99 | -29,35 | -34,41 | -40,87 | -39,77 |
| 10 | | | | | | | | | | -43,5 | -29,86 | -46,27 | -38,17 | -17,89 | -20,17 | -30,76 |
| 11 | | | | | | | | | | | -42,35 | -26,92 | -38,56 | -24,06 | -13,68 | -29,87 |
| 12 | | | | | | | | | | | | -36,99 | -49,38 | -38,53 | -26,68 | -29,87 |
| 13 | | | | | | | | | | | | | -36,22 | -34,42 | -27,34 | -40,79 |
| 14 | | | | | | | | | | | | | | -17,02 | -15,38 | -29,47 |
| 15 | | | | | | | | | | | | | | | -21,84 | -20,98 |
| 16 | | | | | | | | | | | | | | | | -24,71 |

B

| Channel | 1 | 2 | 3 | 4 | 5 | 6 | 7 | 8 | 9 | 10 | 11 | 12 | 13 | 14 | 15 | 16 |
|---|---|---|---|---|---|---|---|---|---|---|---|---|---|---|---|---|
| 1 | -26,2 | -18,01 | -16,01 | -19,64 | -11,04 | -19,98 | -20,32 | -22,09 | -27,19 | -27,67 | -17,4 | -20,77 | -29,15 | -34,58 | -26,01 | -18,95 |
| 2 | | -35,8 | -13,45 | -16,40 | -14,93 | -11,80 | -24,13 | -21,45 | -27,69 | -30,30 | -24,54 | -18,57 | -31,11 | -37,62 | -31,98 | -20,38 |
| 3 | | | -34 | -18,30 | -21,22 | -23,64 | -11,40 | -15,30 | -17,87 | -25,65 | -30,17 | -25,82 | -20,32 | -32,99 | -37,11 | -30,89 |
| 4 | | | | -32,9 | -22,04 | -19,86 | -19,09 | -11,28 | -16,15 | -17,36 | -26,23 | -26,04 | -17,12 | -26,15 | -32,67 | -28,21 |
| 5 | | | | | -27,72 | -19,95 | -13,77 | -23,98 | -29,33 | -28,82 | -23,49 | -16,98 | -27,98 | -44,58 | -24,86 | -14,31 |
| 6 | | | | | | -29,45 | -12,84 | -13,98 | -50,89 | -32,22 | -33,26 | -22,17 | -25,24 | -37,15 | -29,29 | -20,28 |
| 7 | | | | | | | -32,44 | -22,89 | -22,10 | -35,26 | -31,84 | -43,71 | -20,06 | -29,18 | -36,24 | -25,06 |
| 8 | | | | | | | | -33,62 | -15,80 | -23,77 | -27,56 | -27,79 | -14,24 | -24,68 | -42,16 | -27,85 |
| 9 | | | | | | | | | -35,89 | -17,60 | -20,59 | -27,94 | -11,15 | -23,21 | -25,63 | -29,77 |
| 10 | | | | | | | | | | -42,40 | -16,94 | -20,39 | -21,26 | -11,24 | -23,21 | -23,18 |
| 11 | | | | | | | | | | | -40,93 | -17,43 | -23,22 | -23,37 | -11,27 | -20,12 |
| 12 | | | | | | | | | | | | -36,57 | -29,64 | -25,79 | -22,97 | -11,06 |
| 13 | | | | | | | | | | | | | -36,04 | -16,06 | -23,79 | -29,48 |
| 14 | | | | | | | | | | | | | | -17,41 | -19,85 | -24,08 |
| 15 | | | | | | | | | | | | | | | -21,21 | -21,21 |
| 16 | | | | | | | | | | | | | | | | -24,18 |

**FIGURE S2**: Comparison between measured (A) and simulated (B) S-Parameters. Values are obtained from a head-neck agar phantom load. The diagonal elements refer to the S11 matching of the coil, where the S21 off-diagonal show the interelement coupling. The constructed head and neck coil shows slightly more favorable decoupling values in comparison to its simulated version.

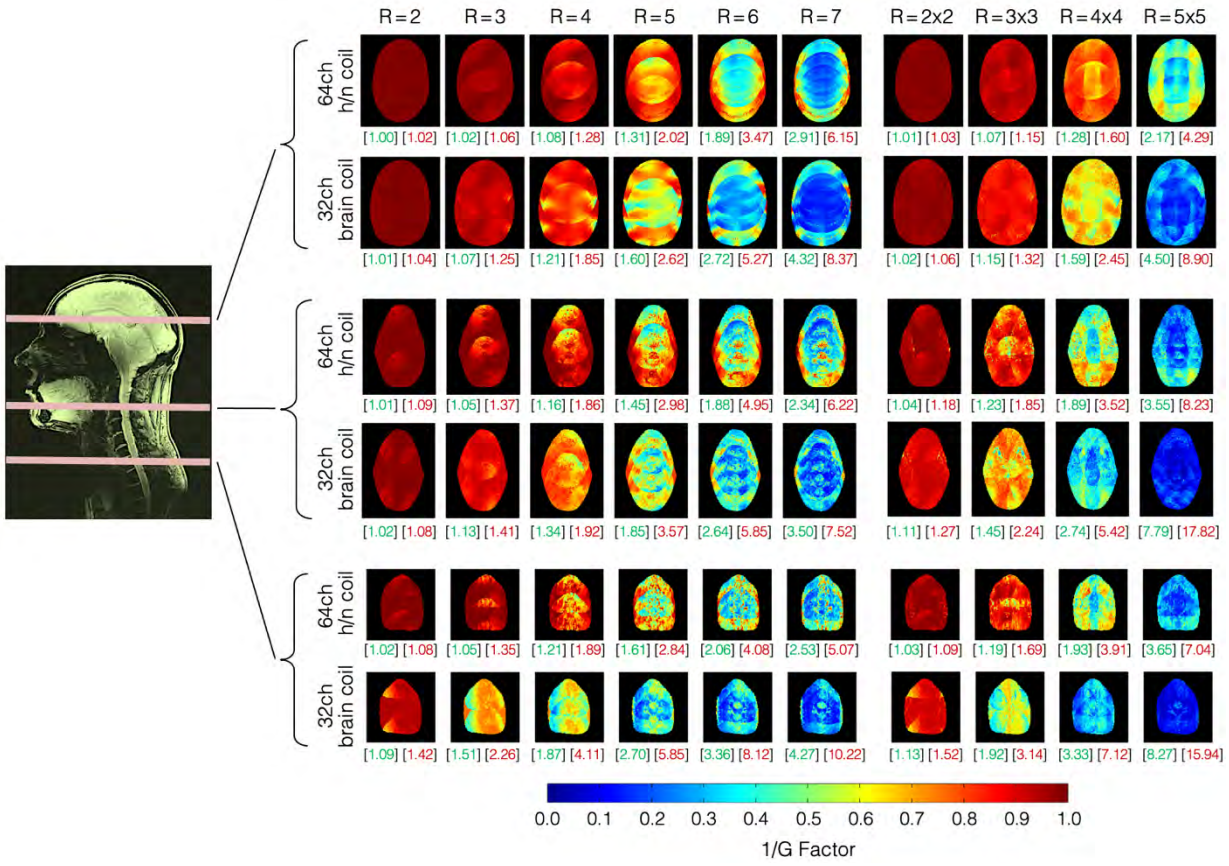


**FIGURE S3**: Inverse G-factors for three transverse slices obtained from the 64-channel head-neck and the 32-channel coils. In the brain region, the 64-channel head-neck coil shows slightly lower noise amplifications at all acceleration stages when compared to the 32-channel head coil. At the neck region, the lower G-factors of the 64-channel coil provide roughly one additional unit of acceleration for a given noise amplification factor when compared to the 32-channel coil. The green and red numbers in brackets indicate the mean and maximum G-factors, respectively (non-inverted values).

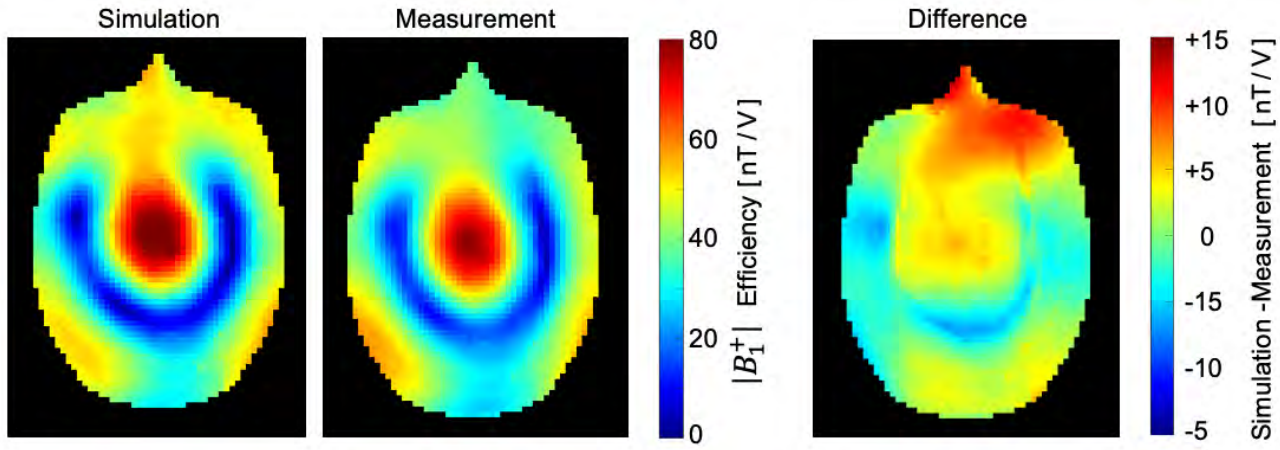


**FIGURE S4**: Comparison of circularly polarized $B_1^+$ efficiency between simulated and measured phantom data obtained in the center of the head-neck coil. Qualitatively, both fields show a good correlation of the field pattern. The simulation shows an 11% better $B_1^+$ efficiency overall. Locally, however, the $B_1^+$ values differ in a range from -7 to + 18 %. Phases for generating the CP mode: Ch1 64°, Ch2 20°, Ch3 340°, Ch4 296°, Ch5 54°, Ch6 18°, Ch7 342°, Ch8 306°, Ch9 249°, Ch10 203°, Ch11 157°, Ch12 111°, Ch13 226°, Ch14 198°, Ch15 162°, Ch16 134°.

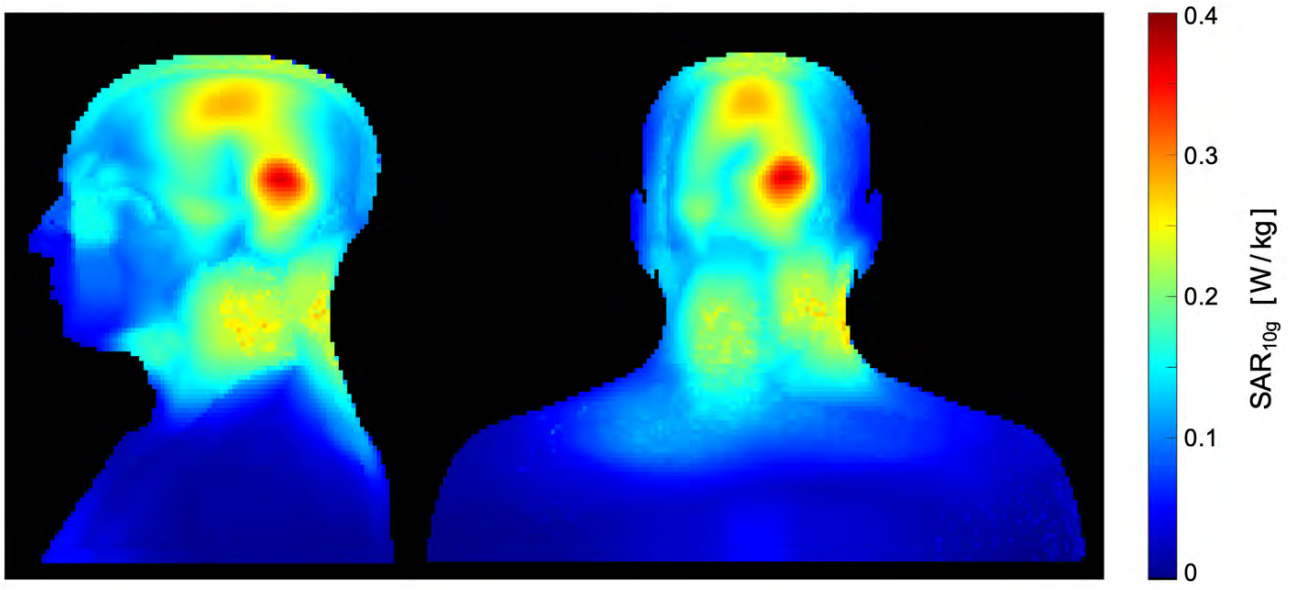


**FIGURE S5**: Simulated SAR10g for the CP mode. Sagittal and coronal slices show a maximum projection map (MIP) of the human multicompartment model. The SAR10g map was acquired with 1W input power for each individual transmit channels. The maximum SAR was measured to be 0.368 W/kg.